Electronic Supplementary Information (ESI)

Enhancement of Chain Rigidity and Gas Transport Performance for Polymers of Intrinsic Microporosity via Intramolecular Locking of the Spiro-carbon

*Jian Zhang, Hong Kang, Jacob Martin, Shouhai Zhang, Sylvie Thomas, Tim C. Merkel and Jianyong Jin**

*To whom correspondence should be addressed. Email: j.jin@auckland.ac.nz

Table of contents

1. Synthetic section

1.1. General methods:

Analytical thin-layer chromatography (TLC) was performed using Kieselgel F254 0.2 mm (Merck) silica plates with visualization by ultraviolet irradiation (254 nm) followed by staining with alkaline potassium permanganate. NMR spectra were recorded on a Bruker DRX400 spectrophotometer. Chemical shifts are reported in parts per million (ppm) referenced to δ 7.26 and 77.0 ppm from chloroform or δ 2.50 and 39.5 ppm from DMSO for ^{1}H and ^{13}C, respectively. The multiplicities of ^{1}H signals are designated by the following abbreviations: s = singlet; d = doublet; dd= doublet of doublets; m = multiplet; br = broad. All ^{13}C NMR spectra were acquired using broadband decoupled mode, and assignments were determined using DEPT sequences. Mass spectra were obtained by ESI using a Bruker micrOTOF-Q mass spectrometer. Molecular weight and molecular weight distributions were determined by PL GPC-50 instrument equipped with 5 mm PL gel Mixed C columns (heated to 40 °C) arranged in series with chloroform as eluent and a RI detector and the values were calibrated versus polystyrene standard. Infrared spectra were recorded on a Perkin Elmer Spectrum 100 FT-IR spectrometer using a diamond ATR sampling accessory.

1.2. Materials:

All chemicals were purchased from Sigma-Aldrich and used as received without further treatment. Except 2,3,5,6-tetrafluoroterephthalonitrile (97%) was purchased from Manchester Organics and recrystallized from ethyl ester before use, and 3-methyl catechol (98%) was purchased from Alfa used as received.

1.3. Synthetic procedures

1.3.1 Synthesis of compound 1[1]

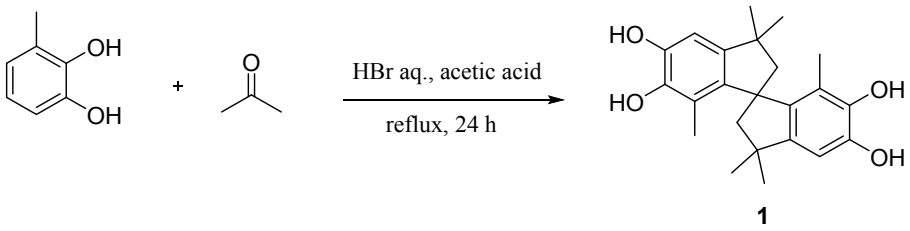

1

To a mixture of conc. HBr aq. (36 mL) and acetic acid (33 mL) was added 1,2-dihydroxy-3methylbenzene (16.8 g, 135 mmol) to give a clear solution. Acetone (21 mL, 286 mmol) was then added dropwise. After addition, the resulting solution was heated to reflux and kept refluxing for 24 h. The hot mixture was poured into water (360 mL) with vigorous stirring. The precipitate was filtered out. Then the solid was stirred in acetic acid (150 mL) for 1 h, filtered, and washed with acetic acid to give compound 1 (15 g, 40.7 mmol, 60%) as an off-white solid. ^{1}H NMR (400MHz, DMSO-d_6): δ ppm 8.83 (br, 2H), 7.67 (br, 2H), 6.43 (s, 2H), 2.16-2.05 (m, 4H), 1.51 (s, 6H), 1.25 (s, 6H), 1.22 (s, 6H); 13C NMR (100MHz, DMSO-d_6): δ ppm 143.95, 142.32, 141.28, 137.46, 119.76, 106.02, 56.96, 56.67, 41.76, 32.54, 29.87, 10.74; HR-MS (ESI) calcd. 391.1880 for $C_{23}H_{28}NaO_4$, found 391.1868 $[M+Na]^+$.

1.3.2 Synthesis of compound 2

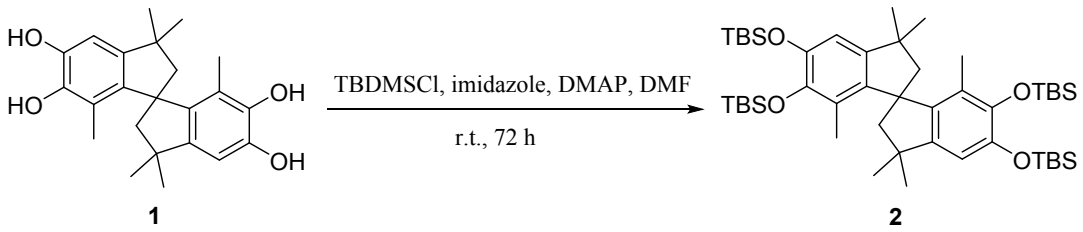

1 2

To a suspension of the biscatechol 1 (10.85 g, 29.4 mmol) in anhydrous DMF (135 mL) was added t-butyl dimethyl silyl chloride (36 g, 239 mmol). The mixture was cooled down in ice-bath and imidazole (24 g, 353 mmol) was added potionwise within 5 min followed by

addition of DMAP (0.36 g, 2.95 mmol). The mixture was stirred under argon atmosphere at room temperature for 3 d. The mixture was poured into methanol (400 mL) and stirred for 1 h. Then, the precipitate was filtered, washed with methanol and dried under vacuum to give compound 2 (22.6 g, 27.4 mmol, 93%) as a white solid. ^{1}H NMR (400MHz, $CDCl_3$): δ ppm 6.48 (s, 2H), 2.24-2.17 (m, 4H), 1.62 (s, 6H), 1.29 (s, 6H), 1.27 (s, 6H), 0.97 (s, 18H), 0.96 (s, 18H), 0.22 (s, 6H), 0.19 (s, 6H), 0.14 (s, 6H), 0.05 (s, 6H); ^{13}C NMR (100MHz, $CDCl_3$): δ ppm 146.21, 144.21, 143.72, 139.96, 125.99, 111.95, 57.90, 56.76, 42.24, 32.69, 29.72, 26.33, 26.27, 18.84, 18.59, 12.73, -3.04, -3.31, -3.68, -3.70; HR-MS (ESI) calcd. 825.5519 for $C_{47}H_{85}O_4Si_4$, found 825.5540 $[M+H]^+$.

1.3.3 Synthesis of compound 3

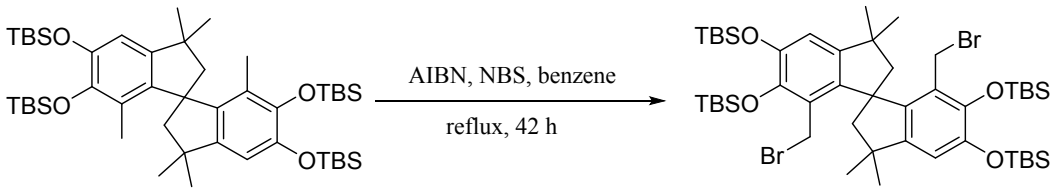

2 **3**

To a solution of compound 2 (10.2 g, 12.4 mmol) in benzene (200 mL) was added NBS (5.50 g, 30.9 mmol), followed by addition of AIBN (200 mg, 0.12 mmol). The mixture was brought to reflux for 42 h. Then, the hot reaction mixture was poured into methanol (2000 mL) to give crystals. The crystals was filtered and washed with methanol to give compound 3 (11.2 g, 11.4 mmol, 92%) as slightly yellowish crystals. ^{1}H NMR (400MHz, $CDCl_3$): δ ppm 6.67 (s, 2H), 4.17 (d, J = 9.6 Hz, 2H), 3.86 (d, J = 9.6 Hz, 2H), 2.71 (d, J = 13.0 Hz, 2H), 2.23 (d, J = 13.0 Hz, 2H), 1.40 (s, 6H), 1.29 (s, 6H), 1.01 (s, 18H), 0.95 (s, 18H), 0.30 (s, 6H), 0.28 (s, 6H), 0.19 (s, 6H), -0.02 (s, 6H); ^{13}C NMR (100MHz, $CDCl_3$): δ ppm 147.26, 145.79, 145.32, 140.76, 126.20, 115.74, 58.64, 55.81, 42.91, 32.78, 30.06, 26.83, 26.54, 26.27, 19.15, 18.76, -2.25, -2.67, -3.65, -4.11; HR-MS (ESI) calcd. 1003.3549 for $C_{47}H_{82}Br_2NaO_4Si_4$, found 1003.3538 $[M+Na]^+$.

1.3.4 Synthesis of monomer 4

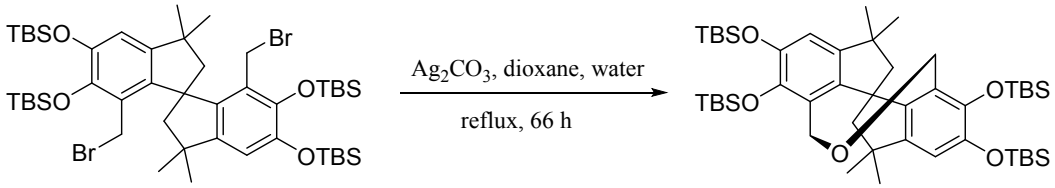

3 **4**

The dibenzylbromide intermediate 3 (2.0 g, 2.04 mmol) and Ag_2CO_3 (2.81 g, 10.2 mmol) were added to a mixture of 1,4-dioxane (94 mL) and water (9.4 mL). Then, the slurry was brought to reflux with effective stirring for 66 h. The mixture was filtered when still hot and the solid was washed with dichloromethane. The filtrate was evaporated to give oily residue. The residual oil was partitioned between water and dichloromethane. The organic layers were combined, dried over anhydrous Na_2SO_4 and evaporated to give crude monomer 4 as a lightly yellow dense oil. The crude product was purified by chromatography (n-hexane/CH_2Cl_2 10:1) to give monomer 4 (0.68 g, 0.81 mmol, 40%) as a colorless dense oil which crystalized soon upon storage. ^{1}H NMR (400MHz, $CDCl_3$): δ ppm 6.58 (s, 2H), 4.62 (d, J = 11.9 Hz, 2H), 4.08 (d, J = 11.9 Hz, 2H), 2.35 (d, J = 12.6 Hz, 2H), 1.86 (d, J = 12.6 Hz, 2H), 1.43 (s, 6H), 1.19 (s, 6H), 0.99 (s, 36H), 0.24 (s, 6H), 0.23 (s, 6H), 0.17 (s, 6H), 0.09 (s, 6H); ^{13}C NMR (100MHz, $CDCl_3$): δ ppm 147.15, 144.08, 143.62, 142.90, 121.70, 114.31, 58.10, 57.85, 56.78, 41.53, 32.39, 30.19, 26.36, 26.25, 18.86, 18.64, -3.34, -3.59, -3.66, -3.98; HR-MS (ESI) calcd. 861.5132 for $C_{47}H_{82}NaO_5Si_4$, found 861.5136 $[M+Na]^+$.

1.3.5 Synthesis of PIM-C1

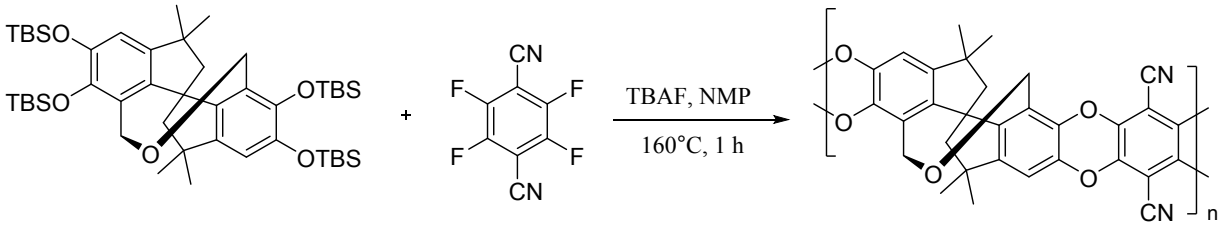

Anhydrous NMP (13.4 mL) was added to a mixture of monomer **4** (1.4974 g, 1.78 mmol) and monomer 2,3,5,6-tetrafluoro-terephthalonitrile (**TFTPN**) (0.3569 g, 1.78 mmol) was added to give a suspension. 1 N TBAF in THF was diluted 10 times with anhydrous NMP. The resulting 0.1 N TBAF solution (0.18 mL, 0.018 mmol) was added to the reaction mixture at room temperature. The reaction mixture was heated to 160 °C gradually for 45 min and kept at 160 °C for 1 h. The mixture was cooled down to room temperature and poured into EtOAc (100 mL) with vigorous stirring for 1 h. The solid was filtered and washed with EtOAc to give crude product which was re-dissolved in $CHCl_3$ and precipitated from MeOH to give **PIM-C1** (0.82 g, 92%) as a yellow solid. ^{1}H NMR (400 MHz, $CDCl_3$, δ): 6.83 (br s, 2H; Ar H), 4.85 (br, 2H; CH_2), 4.12 (br, 2H; CH_2), 2.44(br, 2H; CH_2), 1.95 (br, 2H; CH_2), 1.48 (br s, 6H; CH_3), 1.28 (br s, 6H; CH_3); FT-IR (ATR): v= 2956, 2240, 1436, 1324, 1267, 1047, 1025, 866 cm^{-1}; Anal. calcd for repeating unit [$C_{31}H_{22}N_2O_5$]: C 74.09, H 4.41, N 5.57; found: C 73.39, H 4.44, N 5.53; GPC ($CHCl_3$ as eluent, polystyrene standard): (M_n= 79,000 g mol^{-1}; M_w= 548,000 g mol^{-1}).

1.4. Spectra and figures

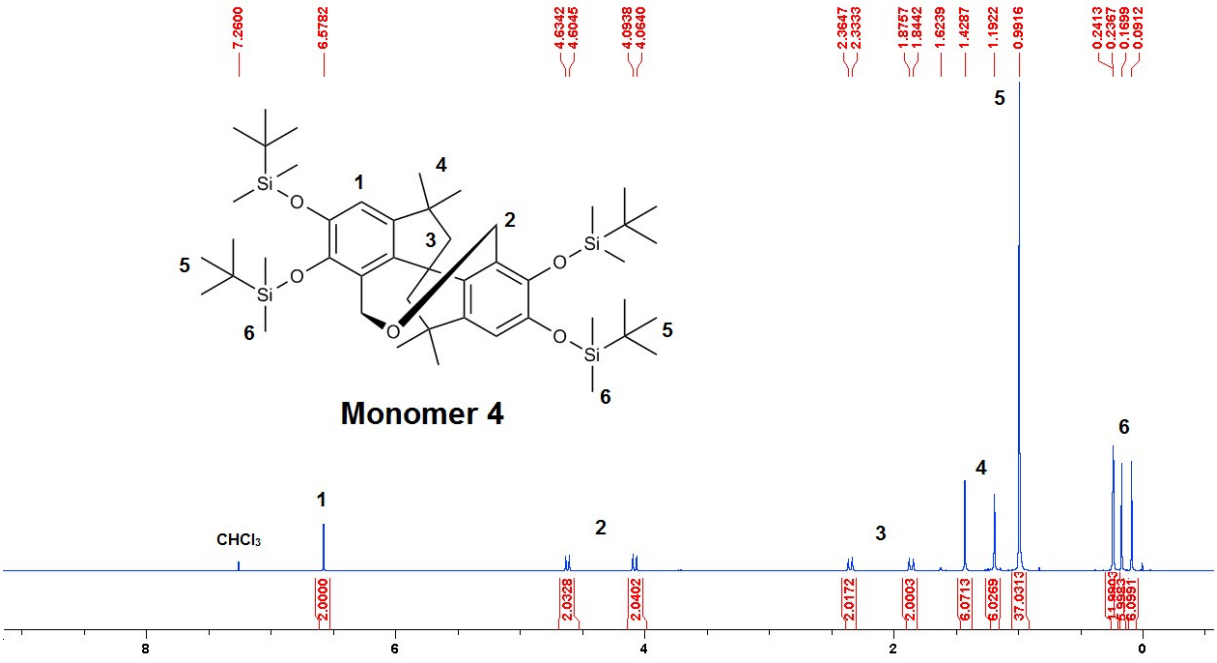

Fig. S1. [1]H NMR spectrum of monomer 4.

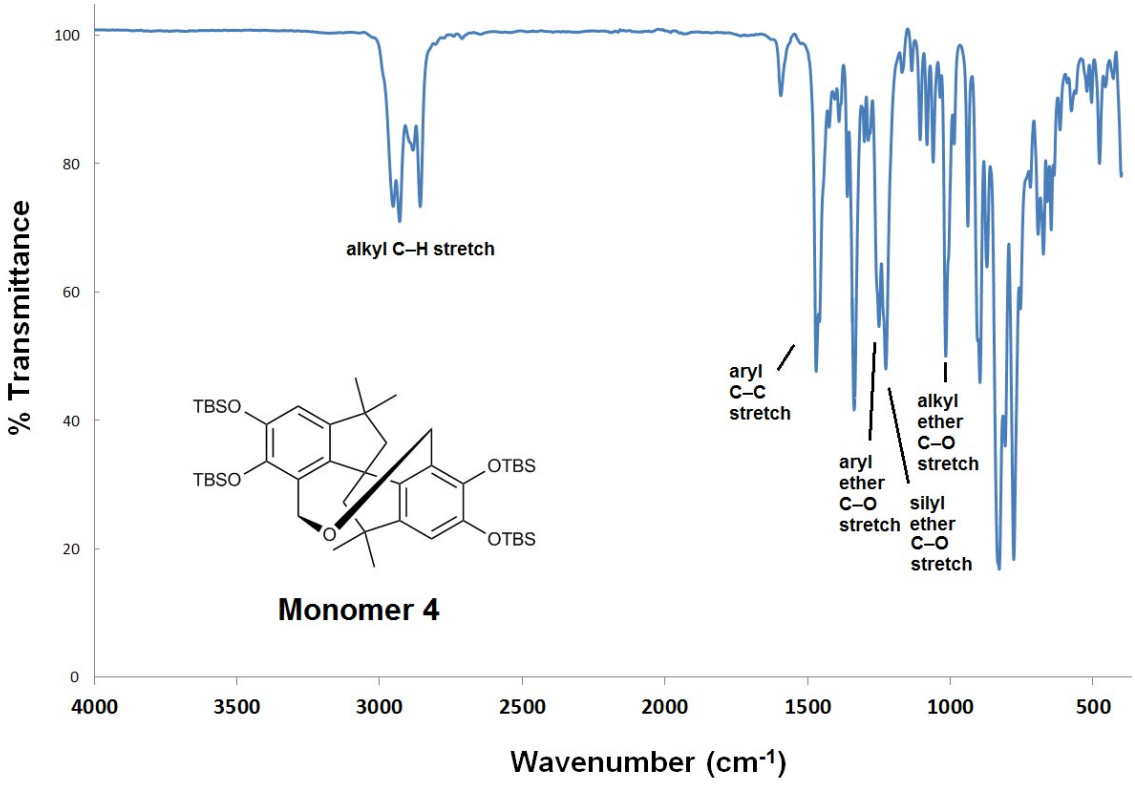

Fig. S2. FT-IR spectrum of monomer 4.

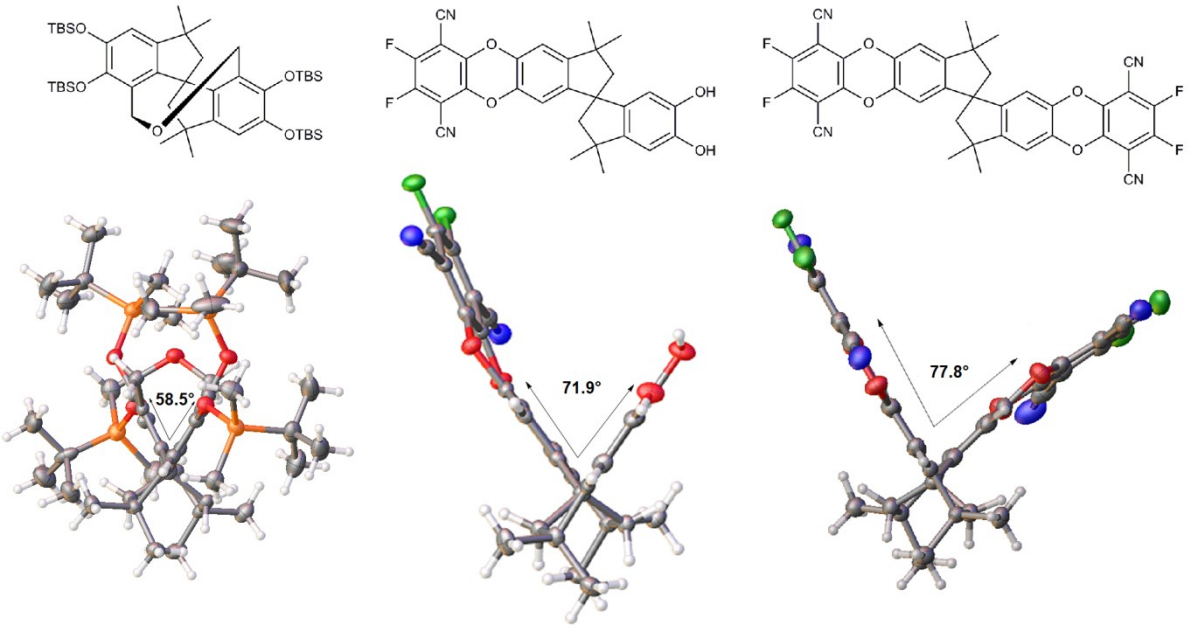

Fig. S3. Comparison of dihedral angles between two benzenes around spiro-center of three spiro-based monomers.[2]

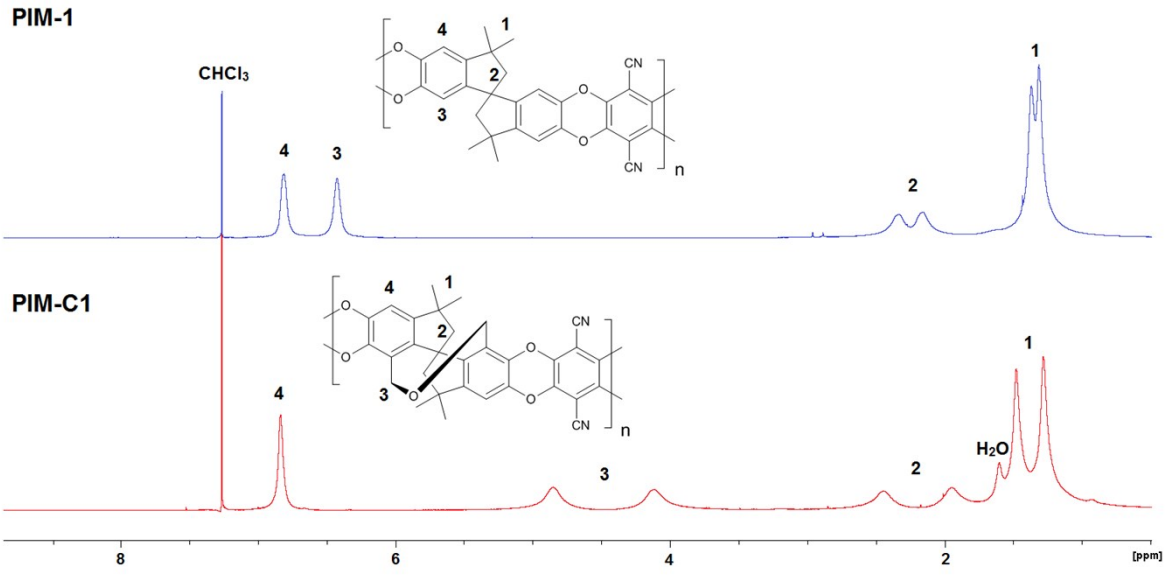

Fig. S4. Comparison of ^{1}H NMR spectra of **PIM-C1** and **PIM-1**.

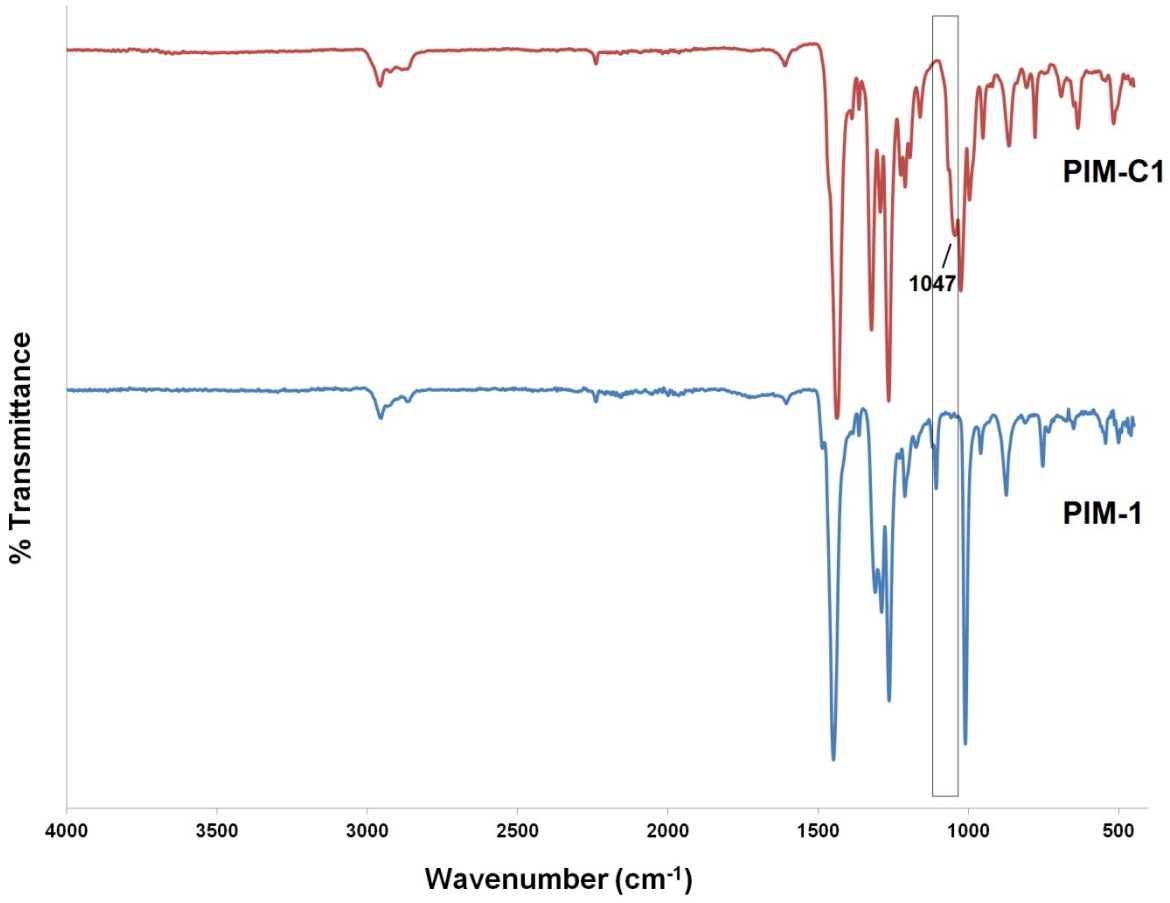

Fig. S5. Comparison of FT-IR spectra of **PIM-C1** and **PIM-1**. The absorption peak of the C-O bond stretch of the dibenzyl ether linkage was marked at 1047 cm^{-1}.

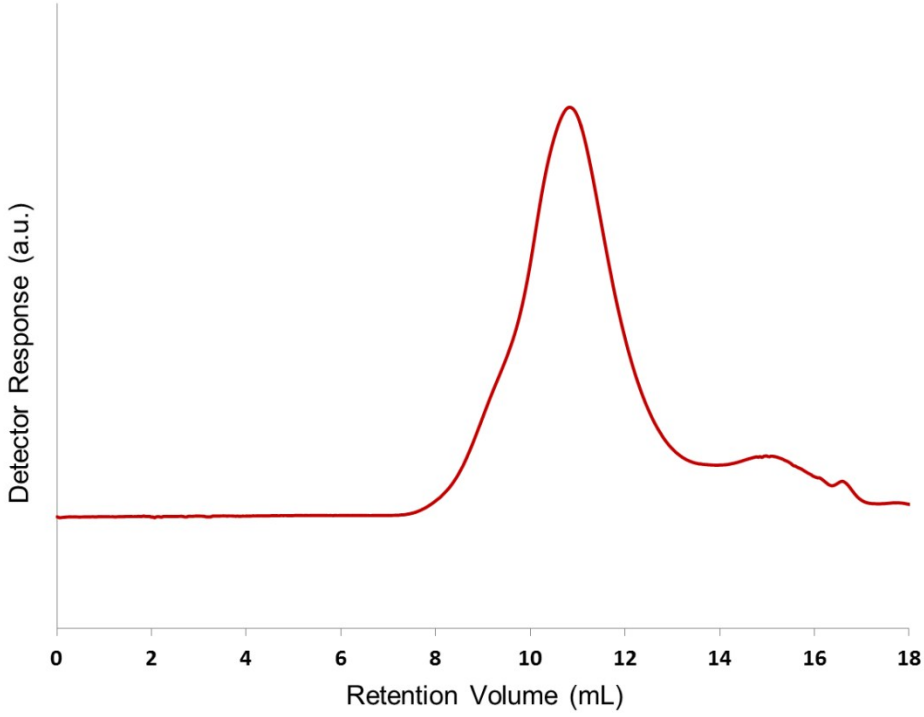

Fig. S6. GPC chromatogram of **PIM-C1**.

2. Modelling section

2.1. Methods

Molecular dynamics simulations were performed using the generalized amber force field (GAFF) which has been used to study **PIM-1** and found to give good representation of the polymer conformation and dynamics. (DOI 10.1080/08927022.2012.733945, 10.3390/membranes5010099) A simplified six unit polymer chain with only the spirobisindane units was constructed in Avogadro and optimized using the UFF force field for an initial conformation. Charges and parameters were taken from Wang et al. (DOI 10.1002/jcc.20035). The software package Abalone was used to perform the simulation and track the end to end chain distance. Each polymer was simulated for 60 ps at 298 K in vacuum with a time step of 0.25 fs. The end to end distance was measured every time step and used to construct the end to end distance histogram.

The dihedral potential energy surface was calculated using B3LYP functional with a 3-21G+ basis set in Gaussian 09. We also performed the calculation using the larger 6-311G+ basis set which gave similar results. The dihedral angles were constrained and scanned in 3 degree increments whilst the geometry was optimized and energy recorded for the different conformers. Igor Pro (WaveMetrics, Lake Oswego, OR, USA) was used to fit of the dihedral angle potential surface below the thermal energy at 25°C (3RT=7.4 kJ mol^{-1}) using a harmonic model as the best approximates $V_D = k_{ijkl}(\phi_{ijkl} - \phi_0)^2$ with k_{ijkl} being taken as the rigidity parameter. The GAFF forcefield led to accessible angles suggested by the DFT calculations.

2.2. Comparison of different modelling methods for the determination of spirobisindane dihedral angle potential energy surface

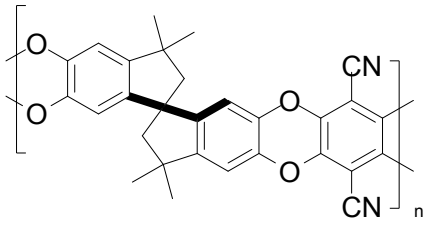

When calculating the potential energy surface of the dihedral angle it is important to use a sufficient level of theory to model the surface, it was found that using the MMFF forcefield a barrier near an angle of ~-58° was found. When modelled using the B3LYP functional using different Gaussian basis sets this barrier was not present. This suggests that a higher level of theory than MMFF is needed to compare different dihedral potential energy surfaces for different moieties and that MMFF over emphasises the steric hindrance caused by the methyl substituting groups around the spiro carbon structure.

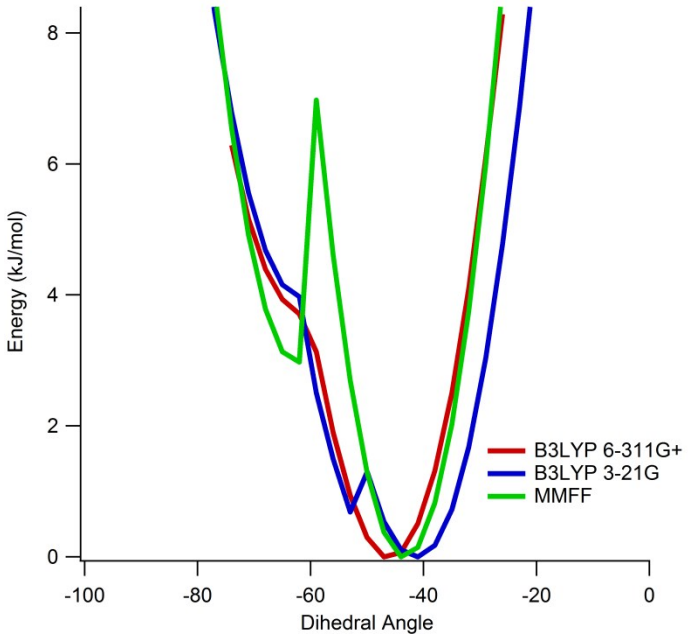

Fig. S7. Dihedral potential energy surface for the SBI structure with different levels of theory. There is a large barrier found for the MMFF simulation in SPARTAN, this is not present in the B3LYP calculations. This suggested there are higher degrees of freedom for the SBI structure than previously thought and highlights the need for at least B3LYP 3-21G to model the potential energy of the structure.

3. Pure gas permeation test conditions and polymer properties

3.1. Methods

TGA Q5000 (TA Instruments) thermal gravimetric analyzer (TGA) was employed to analyze polymer thermal degradation. Samples for TGA study were initially heated to 120 °C and maintained for 30 minutes. under nitrogen flow and then heated to 800 °C at a heating rate of 5 °C min^{-1}. A DSC Q1000 (TA Instruments) differential scanning calorimeter was used to study the glass transition. Samples for DSC was prepared in crimped aluminum sample cell and heated under nitrogen flow to 220 °C then cooled down to 50 °C and re-heated to 400 °C with all heating and cooling processes at a rate of 5 °C min^{-1}. The DSC thermograms were from a second heating after quick cooling. Low-temperature (77 K) nitrogen adsorption measurements were carried out using a TriStar 3000 instrument. Powder samples were degassed at 100 °C overnight. Sartorius YDK 01LP balance equipped with density determination kit was used to determine polymer density. TA.XT plus Texture Analyzer was used in tensile test mode with the test speed of 1.0 mm s^{-1}.

3.2. Pure gas permeation test conditions

Both **PIM-1** and **PIM-C1** were cast into mechanically robust and optically transparent films as shown in Fig. S11. Both films of **PIM-C1** (31μm) and **PIM-1** (65μm) were cast from 2% solution in chloroform by slow evaporation under N_2 current for 2-3 days. Before gas permeation tests, both films were soaked in methanol for 2 h, dried at room temperature for 24 h and then at 65 °C for 1 h. Pure gas permeation tests were conducted at 22°C and at a feed pressure of 50 psig using a constant-pressure, variable-volume apparatus. Experimental results are included in the main text.

Fig. S8. Optically clear films of **PIM-C1** and **PIM-1** for gas permeation measurements.

3.3. BET analysis

Nitrogen sorption isotherms (77 K) were carried out using **PIM-1** and **PIM-C1** powders. The apparent Brunauer–Emmett–Teller (BET) surface area of **PIM-C1** is 818 m^2 g^{-1}, which is 11% higher than that of **PIM-1** (739 m^2 g^{-1}).

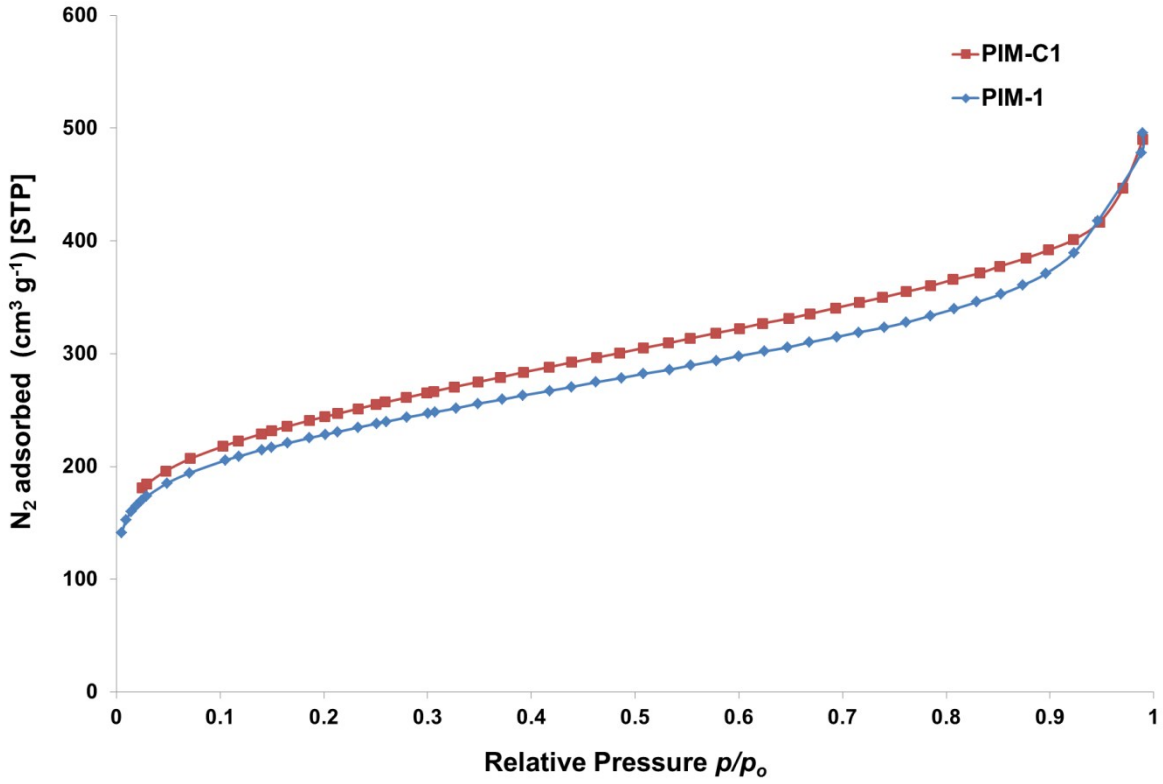

Fig. S9. Nitrogen adsorption isotherms measured for **PIM-C1** and **PIM-1** at 77 K. Saturation pressure, p_o = 1 bar.

3.4. Mechanical properties of PIM-C1 film

The mechanical strength of a **PIM-C1** isotropic film (94 μm thickness) was tested to determine tensile strength at break (MPa) and elongation at break (%). The measured values are 47.2 MPa and 8.4%, respectively, which are close to those reported for **PIM-1**.[4] A TA.XT plus Texture Analyzer was used in tensile test mode with the test speed of 1.0 mm/sec.

Table S1. Mechanical properties of **PIM-C1** film

Polymers	Tensile strength (MPa)	Elongation at break (%)
PIM-1[4]	48	10
PIM-C1	47.22±1.04	8.44±0.74

Details on the calculation

Sample 1:

Thickness of the film: 94 μm

Width of the film at the point of break: 10.5 mm

Initial length: 30.0 mm

Force at break: 47.78868 N

Elongation at break: (22.058 mm – 19.278 mm)/ 30 mm = 9.27%

Tensile strength: 47.78868 N/ (10.5 mm * 0.094 mm) = 48.42 MPa

Sample 2:

Thickness of the film: 94 μm

Width of the film at the point of break: 10.0 mm

Initial length: 30.0 mm

Force at break: 43.74471 N

Elongation at break: (21.522 mm - 19.162 mm)/ 30 mm = 7.87%

Tensile strength: 43.74471 N/ (10.0 mm * 0.094 mm) = 46.54 MPa

Sample 3:

Thickness of the film: 112 μm

Width of the film at the point of break: 10.0 mm

Initial length: 16.5 mm

Force at break: 52.32069 N

Elongation at break: (5.918 mm - 4.569 mm)/ 16.5 mm = 8.18%

Tensile strength: 52.32069 N/ (10.0 mm * 0.112 mm) = 46.71 MPa

3.5. Density test of PIM-C1 film

The density of **PIM-C1** was measured to be 1.065 g cm^{-3} which is close to but slightly lower than the density of **PIM-1** (1.09 g cm^{-3}).[3] A Sartorius YDK 01LP balance equipped with a density determination kit was used to determine the weight of the film in air and in water. The mean and standard deviation of density of **PIM-C1** are listed in the table below compared with reported density of **PIM-1**.

Table S2. Density of **PIM-C1** film

Polymers	Density (g cm^{-3})
PIM-1[3]	1.09
PIM-C1	1.065±0.02

Details on the calculation

Sample 1: #1 Temperature 18.9° ρ_{H2O}=0.99845 g/cm^3

Weight in air 0.0499 g

Weight in water 0.0032 g

ρ_{PIM-C1}= 1.067 g cm^{-3}

Sample 1: #2 Temperature 19.0° ρ_{H2O}=0.99843 g cm^{-3}

Weight in air 0.0502 g

Weight in water 0.0044 g

ρ_{PIM-C1}= 1.092 g cm^{-3}

Sample 1: #3 Temperature 19.2° ρ_{H2O}=0.99839 g cm^{-3}

Weight in air 0.0503 g

Weight in water 0.0026 g

$\rho_{PIM\text{-}C1}$= 1.053 g cm^{-3}

Sample 2: #4 Temperature 19.2° ρ_{H2O}=0.99839 g cm^{-3}

Weight in air 0.0284 g

Weight in water 0.0013 g

$\rho_{PIM\text{-}C1}$= 1.046 g cm^{-3}

3.6. TGA and DSC results

Thermogravimetric analysis (TGA) and differential scanning calorimetry (DSC) were used to characterize the thermal properties of **PIM-C1**. An excellent thermal stability was suggested with onset decomposition temperature at 421°C, which is slightly lower than that of **PIM-1** (436°C, tested in this work) (Fig. S8). According to DSC results, no discernible T_g was observed in the measured range of 50-400°C for both **PIM-C1** and **PIM-1** (Fig. S9).

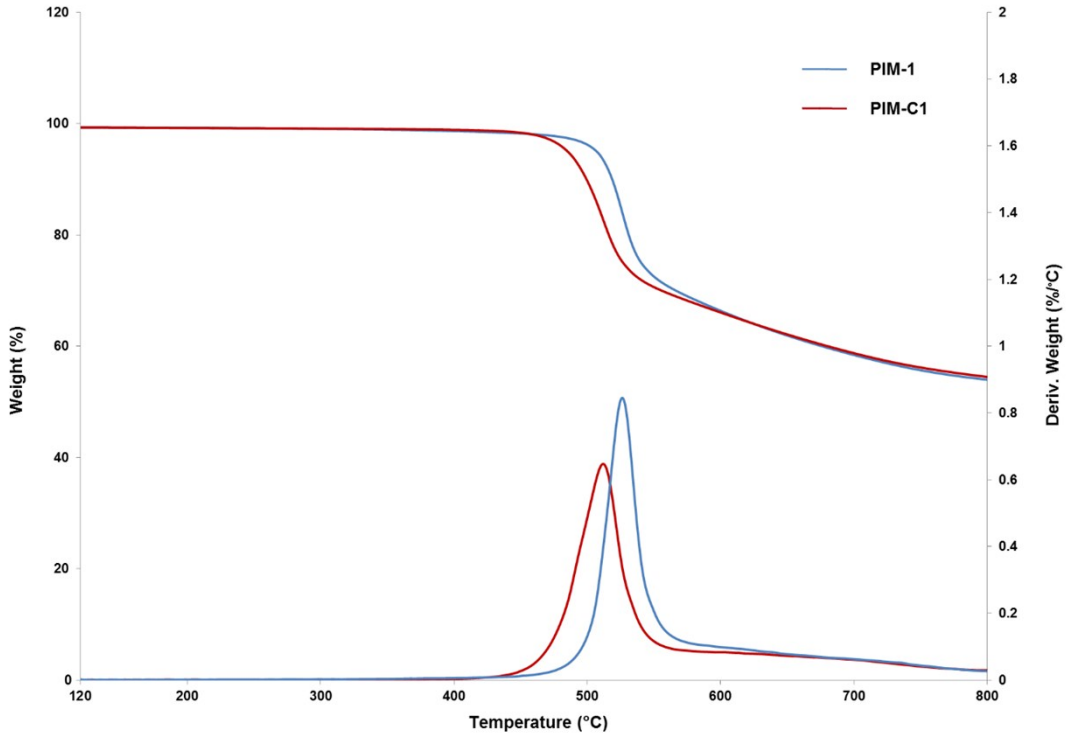

Fig. S10. Comparison of thermogravimetric analysis thermograms (TGA) results of **PIM-C1** and **PIM-1**.

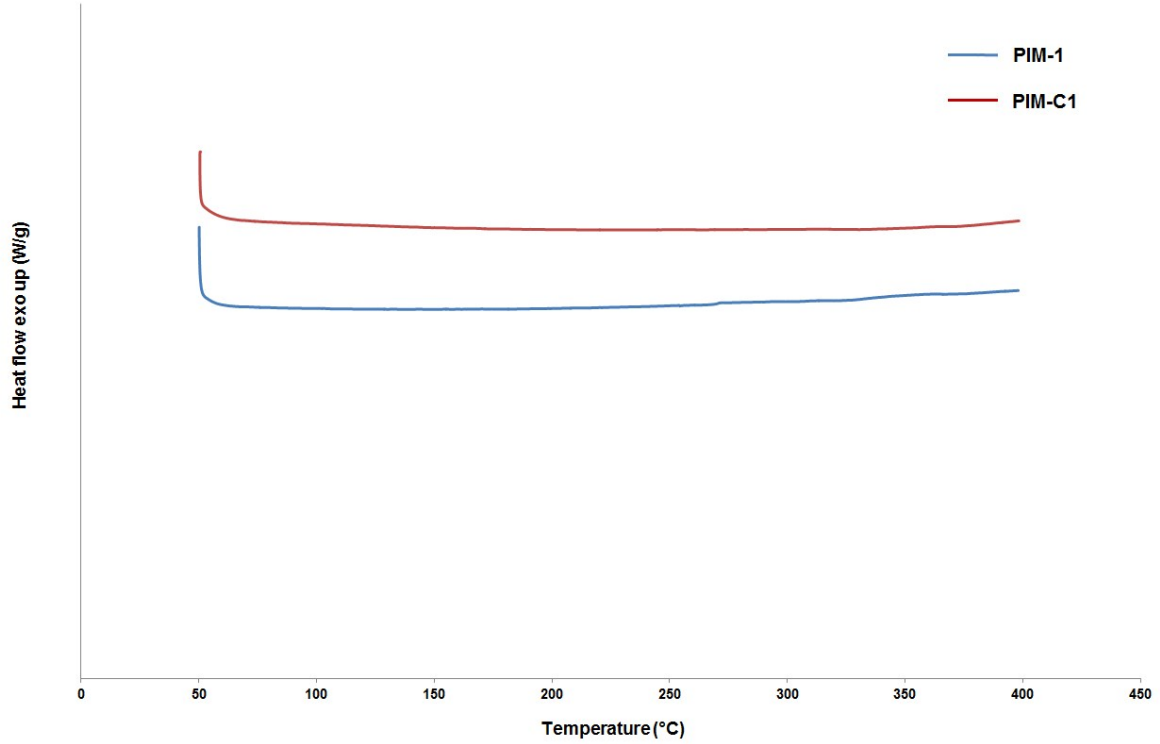

Fig. S11. Comparison of differential scanning calorimetry (DSC) results of **PIM-C1** and **PIM-1**.

References

1. D. Fritsch, G. Bengtson, M. Carta, N. B. McKeown, *Macromol. Chem. Phys.* **2011**, *212*, 1137.

2. a) J. Zhang, J. Jin, R. Cooney, S. Zhang, *Polymer* **2015**, *57*, 45; b) J. Zhang, J. Jin, R. Cooney, Q. Fu, G. G. Qiao, S. Thomas, T. C. Merkel, *Polym. Chem.* **2015**, *6*, 5003.

3. M. Heuchel, D. Fritsch, P. M. Budd, N. B. McKeown, D. Hofmann, *J. Membr. Sci.* **2008**, *318*, 84.

4. a) N. Du, G. P. Robertson, I. Pinnau, M. D. Guiver, *Macromolecules* **2010**, *43*, 8580; b) N. Du, G. P. Robertson, J. Song, I. Pinnau, S. Thomas, M. D. Guiver, *Macromolecules* **2008**, *41*, 9656.